

Effects of Sr substitution on dimensionality and superconducting properties of $\text{Hg}_{0.7}\text{Pb}_{0.3}\text{Ba}_2\text{Ca}_2\text{Cu}_3\text{O}_y$

Yi Zhuo,* Su-Mi Oh, Jae-Hyuk Choi, Mun-Seog Kim, and Sung-Ik Lee

National Creative Research Initiative Center for Superconductivity, Department of Physics, Pohang University of Science and Technology, Pohang 790-784, Korea

N. P. Kiryakov, M. S. Kuznetsov, and Sergey Lee

Department of Chemistry, Moscow State University, Moscow 119899, Russia

(Received 13 April 1999)

The effects of Sr substitution on the Ba site for $\text{Hg}_{0.7}\text{Pb}_{0.3}\text{Ba}_2\text{Ca}_2\text{Cu}_3\text{O}_y$ superconductors were studied. The irreversibility line for the Sr-substituted compound is much steeper compared to the pristine sample. From the analysis of the reversible magnetization, we found that the fluctuation magnetization is much suppressed in the Sr-substituted compound, though the high-field magnetization data around $T_c(H)$ still displayed two-dimensional scaling behavior. This feature can be explained by the enhanced interlayer coupling strength associated with the Sr substitution. Various thermodynamic parameters were obtained from the theoretical analysis. It is notable that the zero-temperature upper critical field $H_{c_2}(0)$ of the Sr-substituted sample is about two times that of the nonsubstituted sample. [S0163-1829(99)02633-8]

I. INTRODUCTION

In Hg-based superconductors, $\text{HgBa}_2\text{Ca}_{n-1}\text{Cu}_n\text{O}_{2n+2}$ ($n = 1-6$), $\text{HgBa}_2\text{Ca}_2\text{Cu}_3\text{O}_{8+\delta}$ (Hg-1223) has the highest superconducting transition temperature with $T_c = 134$ K at ambient pressure, and 164 K under high pressure.¹ Despite their attractive high T_c , there exist some difficulties in practical use because of their complexity in synthesis, chemical instability, and the weak flux-pinning behavior.² Chemical substitution could be a very effective pathway to overcome these problems. Partial substitution of Hg by Pb can stabilize the Hg-1223 structure and increase the T_c of as-prepared samples.³⁻⁵ In addition, partial substitution of Hg by Re greatly enhances the chemical stability and the flux-pinning properties of Hg-1223.⁶

The flux-pinning behavior of a superconductor is characterized by means of the irreversibility line. The irreversibility line separates the irreversible region from the reversible region in the $H-T$ phase diagram. The irreversibility line $H_{\text{irr}}(T)$ of Hg-1223 lies between those of $\text{YBa}_2\text{Cu}_3\text{O}_{7-\delta}$ (Y-123) and $\text{Bi}_2\text{Sr}_2\text{Ca}_1\text{Cu}_2\text{O}_{8+\delta}$ (Bi-2212) superconductors.² The substitution of Ba by the smaller Sr cation in $\text{HgBa}_2\text{O}_{2-\delta}$ charge reservoir block leads to a decrease of the distance between the superconducting CuO_2 blocks, which may enhance the interlayer coupling strength and cause a shift of the irreversibility line to higher fields.⁷⁻⁹ In addition, the Sr-substituted Hg(Pb)-1223 compounds can be easily synthesized by a simple encapsulation technique without using a dry box and possess excellent chemical stability.¹⁰

In order to understand the roles of Sr substitution on the Ba site better in Hg-1223 compound, we measured the magnetization of grain-aligned $\text{Hg}_{0.7}\text{Pb}_{0.3}\text{Ba}_2\text{Ca}_2\text{Cu}_3\text{O}_y$ and $\text{Hg}_{0.7}\text{Pb}_{0.3}\text{Sr}_2\text{Ca}_2\text{Cu}_3\text{O}_y$ samples. The influence of Sr substitution on the lattice parameter, the superconducting dimensionality, the fluctuation effect, the irreversibility line, and the thermodynamic parameters were investigated.

II. EXPERIMENTS

The starting precursor powders were obtained by spray drying of the nitrate solutions. Nitrate solutions with different compositions, $\text{Ba}_2\text{Ca}_2\text{Cu}_3\text{O}_y$ and $\text{Sr}_2\text{Ca}_2\text{Cu}_3\text{O}_y$, were prepared by dissolution of BaCO_3 (or SrCO_3), CaCO_3 , and CuO in high-purity HNO_3 . Thermal decomposition of the nitrate mixtures was carried out in a vacuum at the heating rate of 100°C/h with the maximum temperature at 650°C for 1 hour.

The obtained precursors were mixed with the HgO and PbO. Compacted pellets were placed in an alumina crucible and separated by MgO plates to prevent interaction and then inserted into quartz ampoules. Heat treatment was carried out in evacuated quartz ampoules at 850°C for 5–15 h. The details of the sample preparation were described previously.¹⁰

To obtain a c -axis aligned sample, the powder was ground down to around $20\ \mu\text{m}$ and mixed with epoxy, then cured in a magnetic field of 7 T for 10 h at room temperature. The magnetic measurement was performed in a superconducting quantum interference device magnetometer (MPMS, Quantum Design). The background contribution from the epoxy and the sample holder was carefully subtracted by fitting the magnetization data in the high-temperature region of $200 \leq T \leq 250$ K.

III. RESULTS AND DISCUSSION

Figure 1 shows the temperature dependence of low-field susceptibility in the c -axis direction. The superconducting transition temperatures are 127 and 110 K for $\text{Hg}_{0.7}\text{Pb}_{0.3}\text{Ba}_2\text{Ca}_2\text{Cu}_3\text{O}_y$ and $\text{Hg}_{0.7}\text{Pb}_{0.3}\text{Sr}_2\text{Ca}_2\text{Cu}_3\text{O}_y$, respectively.

Figure 2 shows the x-ray powder-diffraction pattern for both samples. All peaks in the pattern correspond to the $(00l)$ reflections of the Hg-1223 phase, which indicates an

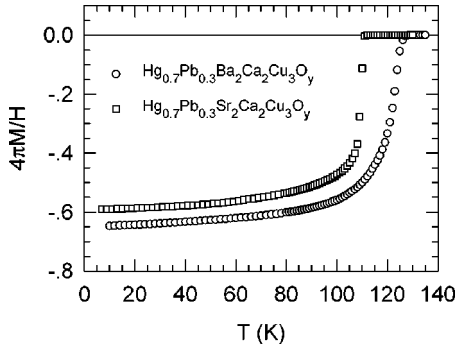


FIG. 1. Temperature dependence of susceptibility in the c -axis direction.

excellent alignment. The c -axis lattice parameter is calculated from the x-ray-diffraction data, with $c = 15.9 \text{ \AA}$ for the pristine, and $c = 15.2 \text{ \AA}$ for the Sr-substituted sample. The substitution of Sr for Ba shortens the c -axis lattice parameter by about 0.7 \AA . The decrease of the c -axis lattice parameter is consistent with the results ($0.8\text{--}0.9 \text{ \AA}$) of Chmaissem *et al.*¹¹

As reported previously, the reduction of the c -axis parameter occurs mainly due to the compression of the $\text{HgBa}_2\text{O}_{2-\delta}$ charge reservoir block for Sr-substituted samples.⁹ The interlayer coupling can be improved by shortening the thickness of the charge reservoir block. It has been reported that the coupling strength between superconducting CuO_2 planes is exponentially reduced with increasing interlayer distance.^{7,12} The fluctuation grows rapidly as the interlayer coupling is reduced, which results in a steady progression from relatively weak three-dimensional (3D) fluctuation to strong 2D fluctuation over a wide temperature range. The interlayer coupling decreases from Y-123, through Hg-1223, to Bi-2212. It was generally accepted that Y-123 is a 3D superconductor and Bi-2212 has a 2D character. Although it is controversial, it is believed that the dimensionality of Hg-1223 is between that of Y-123 and Bi-2212. Thus it is quite interesting to investigate the dimensionality of the Sr-substituted compound.

The reversible magnetization for the high fields from 1–5 T is shown in Fig. 3. The crossover of the magnetization is observed about 2 K below T_c , which is due to the vortex fluctuation effect.

In the high-field limit, according to Ullah and Dorsey,¹³ the magnetization in the critical region is described by the

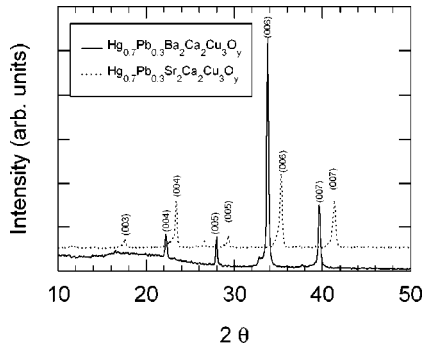


FIG. 2. X-ray-diffraction pattern for grain-aligned $\text{Hg}_{0.7}\text{Pb}_{0.3}\text{Ba}_2\text{Ca}_2\text{Cu}_3\text{O}_y$ and $\text{Hg}_{0.7}\text{Pb}_{0.3}\text{Sr}_2\text{Ca}_2\text{Cu}_3\text{O}_y$.

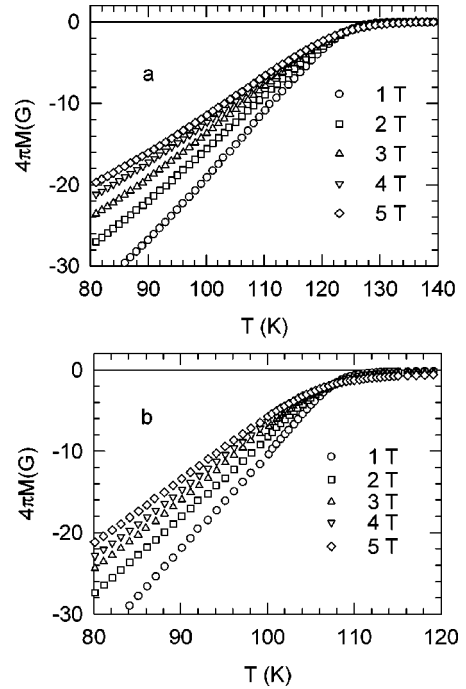


FIG. 3. Temperature dependence of reversible magnetization $4\pi M(T)$ with applied field parallel to the c axis. (a) $\text{Hg}_{0.7}\text{Pb}_{0.3}\text{Ba}_2\text{Ca}_2\text{Cu}_3\text{O}_y$; (b) $\text{Hg}_{0.7}\text{Pb}_{0.3}\text{Sr}_2\text{Ca}_2\text{Cu}_3\text{O}_y$.

scaling law with variable $A[T - T_c]/(TH)^n$. For the fluctuation magnetization, the scaling law is expressed by¹³

$$\frac{4\pi M}{(TH)^n} = F \left[A \frac{T - T_c(H)}{(TH)^n} \right], \quad (1)$$

where F is a scaling function, A is a temperature and field independent coefficient, and the exponent n is $2/3$ for 3D and $1/2$ for 2D. For the two compounds, as shown in Fig. 4, the magnetization data at different external fields collapsed into a universal curve of 2D scaling form. From this analysis, the upper critical field slope $(dH_{c2}/dT)_{T_c}$ was estimated to be -1.4 T/K for the pristine and -2.8 T/K for the Sr-substituted sample. The $(dH_{c2}/dT)_{T_c}$ of the Sr-substituted sample is two times that of the nonsubstituted sample. We also tried to scale our magnetization data into 3D form, but the fitting was rather poor. From the above scaling behavior, it is believed that $\text{Hg}_{0.7}\text{Pb}_{0.3}\text{Ba}_2\text{Ca}_2\text{Cu}_3\text{O}_y$ has a strong two-dimensional superconducting character. Meanwhile, it became clear that $\text{Hg}_{0.7}\text{Pb}_{0.3}\text{Sr}_2\text{Ca}_2\text{Cu}_3\text{O}_y$ still has a 2D nature, although the substitution of Ba by Sr causes a shorter c -axis lattice parameter.

The 2D character of the Sr-substituted sample could also be proved in the analysis based on the vortex fluctuation model. For highly anisotropic layered superconductors, the interlayer interaction between the CuO_2 planes is weak and the positional fluctuation of the vortex is significant, which is reflected by the crossover of the magnetization. This nature is obvious for highly anisotropic Bi- or Tl-based superconductors. As shown in Fig. 3, the crossover of magnetization is observed in both the Sr-free and Sr-substituted samples. If

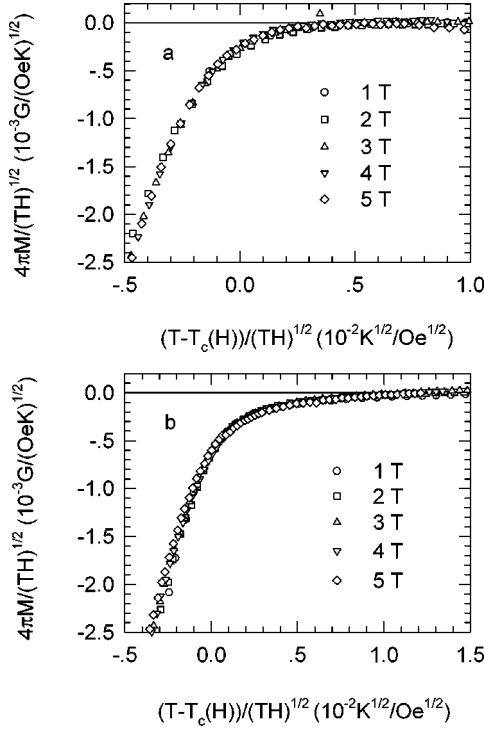


FIG. 4. 2D scaling of the magnetization in the high fields. (a) $\text{Hg}_{0.7}\text{Pb}_{0.3}\text{Ba}_2\text{Ca}_2\text{Cu}_3\text{O}_y$; (b) $\text{Hg}_{0.7}\text{Pb}_{0.3}\text{Sr}_2\text{Ca}_2\text{Cu}_3\text{O}_y$.

the contribution from the positional fluctuation of vortices is included in the total free energy, the derivative of magnetization is given as¹⁴

$$\frac{\partial M}{\partial \ln H} = \frac{\phi_0}{32\pi^2 \lambda_{ab}^2(T)} [1 - g(T)], \quad (2)$$

where s is the effective interlayer spacing and $g(T)$ is defined as

$$g(T) = \frac{32\pi^2 k_B}{\phi_0^2 s} T \lambda_{ab}^2(T). \quad (3)$$

Figure 5 shows the temperature dependence of the slope $\partial M/\partial \ln H$. The solid line represents the values from Eq. (2) assuming the BCS clean limit for $\lambda_{ab}(T)$. The experimental data are in good agreement with theoretical values for both samples. From this analysis, $\lambda_{ab}(0) = 199$ nm and $s = 59$ Å are obtained for the pristine sample, and 158 nm and 43 Å for the Sr-substituted sample.

The s value is rather larger than the crystallographic interlayer spacing determined by the x-ray-diffraction method. This deviation was observed in other 2D-like superconductors, and was explained by using a theoretical result from Koshelev.¹⁵ Therefore the Sr-substituted compound, $\text{Hg}_{0.7}\text{Pb}_{0.3}\text{Sr}_2\text{Ca}_2\text{Cu}_3\text{O}_y$, is a 2D superconductor although the substitution of Ba by Sr causes a shorter c -axis lattice parameter.

The above result indicates that the Sr substitution does not change the superconducting dimensionality. In order to study the effects of Sr substitution on the fluctuation, the Hao-Clem model was used to analyze the reversible magnetiza-

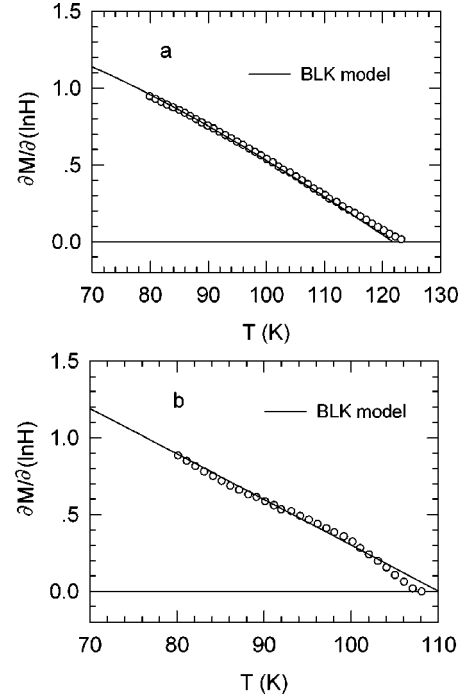


FIG. 5. Temperature dependence of the slope $\partial M/\partial \ln H$. Solid lines represent theoretical fitting. (a) $\text{Hg}_{0.7}\text{Pb}_{0.3}\text{Ba}_2\text{Ca}_2\text{Cu}_3\text{O}_y$; (b) $\text{Hg}_{0.7}\text{Pb}_{0.3}\text{Sr}_2\text{Ca}_2\text{Cu}_3\text{O}_y$.

tion. The Hao-Clem model, as a mean-field model, does not consider the fluctuation effect. Therefore its application to the region where the fluctuation dominates gives the obtained Ginzburg-Landau parameter $\kappa(T)$ deviating from the real value. This deviation reflects the strength of fluctuation and was used as a tool to find the fluctuation-dominant region.

A detailed description of this approach is given in Ref. 16. The Ginzburg-Landau parameter $\kappa(T)$ and thermodynamic critical field $H_c(T)$ were obtained from this analysis. As shown in Fig. 6, the temperature dependence of $\kappa(T)$ is different for $\text{Hg}_{0.7}\text{Pb}_{0.3}\text{Ba}_2\text{Ca}_2\text{Cu}_3\text{O}_y$ and $\text{Hg}_{0.7}\text{Pb}_{0.3}\text{Sr}_2\text{Ca}_2\text{Cu}_3\text{O}_y$. For the pristine sample, the $\kappa(T)$ increases slowly with increasing temperatures up to 110 K, then anomalously increases above 110 K ($T/T_c = 0.86$), which is very similar to the behavior of $\text{HgBa}_2\text{Ca}_2\text{Cu}_3\text{O}_y$ and $\text{Hg}_{0.8}\text{Pb}_{0.2}\text{Ba}_{1.5}\text{Sr}_{0.5}\text{Ca}_2\text{Cu}_3\text{O}_y$ compounds.^{17,18} In contrast, the κ of the Sr-substituted sample decreases weakly with temperature in the range $92 \leq T \leq 100$ K, and the anomalous behavior is limited to a very narrow temperature region, $T/T_c \geq 0.95$.

For the Sr-substituted sample, the temperature range with the unusual behavior of κ near T_c is significantly narrower than that of $\text{Hg}_{0.7}\text{Pb}_{0.3}\text{Ba}_2\text{Ca}_2\text{Cu}_3\text{O}_y$. These behaviors imply that the fluctuation effect is severe in the pristine sample, and is obviously suppressed in the Sr-substituted sample although $\text{Hg}_{0.7}\text{Pb}_{0.3}\text{Sr}_2\text{Ca}_2\text{Cu}_3\text{O}_y$ is still a 2D superconductor. The suppression of fluctuation may be attributed to the enhanced interlayer coupling due to the compression of the charge reservoir block between the superconducting CuO_2 planes in the Sr-substituted sample.

In order to study the effect of Sr substitution on the thermodynamic parameters, the relatively low-temperature ranges, $90 \leq T \leq 110$ K for $\text{Hg}_{0.7}\text{Pb}_{0.3}\text{Ba}_2\text{Ca}_2\text{Cu}_3\text{O}_y$ and 90

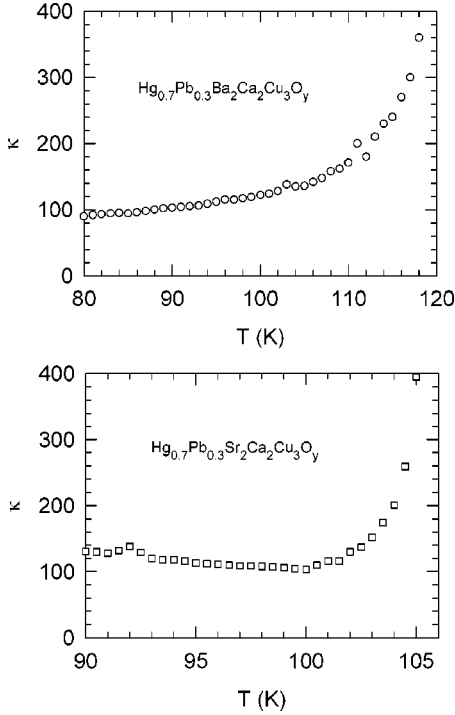


FIG. 6. Temperature dependence of the Ginzburg-Landau parameter $\kappa(T)$ obtained from the Hao-Clem model.

$\leq T \leq 102$ K for $\text{Hg}_{0.7}\text{Pb}_{0.3}\text{Sr}_2\text{Ca}_2\text{Cu}_3\text{O}_y$, are chosen since the obtained κ value is influenced by the thermal fluctuation. In this temperature range, the fluctuation is significantly suppressed. Therefore the change of $\kappa(T)$ with temperature is small and the average value is meaningful in this region. As shown in Fig. 7, the experimental data is well described by

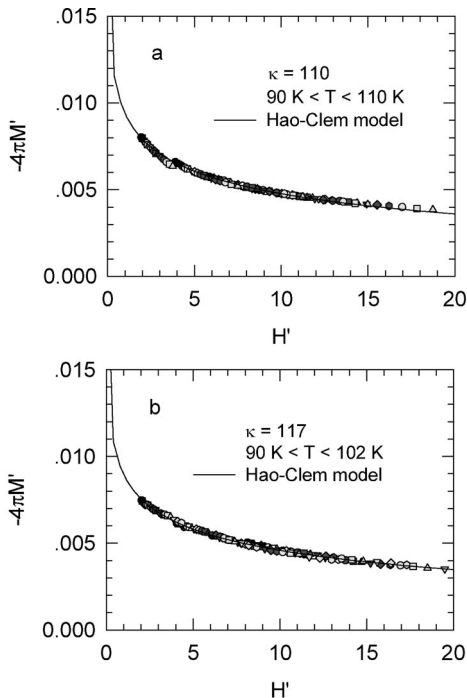


FIG. 7. Magnetization vs applied field scaled by $\sqrt{2}H_c(T)$. Solid line represents the theoretical curve from the Hao-Clem model. (a) $\text{Hg}_{0.7}\text{Pb}_{0.3}\text{Ba}_2\text{Ca}_2\text{Cu}_3\text{O}_y$; (b) $\text{Hg}_{0.7}\text{Pb}_{0.3}\text{Sr}_2\text{Ca}_2\text{Cu}_3\text{O}_y$.

TABLE I. Thermodynamic parameters of $\text{Hg}_{0.7}\text{Pb}_{0.3}\text{Ba}_2\text{Ca}_2\text{Cu}_3\text{O}_y$ and $\text{Hg}_{0.7}\text{Pb}_{0.3}\text{Sr}_2\text{Ca}_2\text{Cu}_3\text{O}_y$ from the theoretical analysis.

	$\text{Hg}_{0.7}\text{Pb}_{0.3}\text{Ba}_2\text{Ca}_2\text{Cu}_3\text{O}_y$	$\text{Hg}_{0.7}\text{Pb}_{0.3}\text{Sr}_2\text{Ca}_2\text{Cu}_3\text{O}_y$
T_c (K)	127 (low field) 129 (BCS result)	110 111
κ	110	117
$H_{c2}(0)$ (T)	0.8	1.1
$\lambda_{ab}(0)$ (nm)	191	169
	199 (BLK)	158
$(dH_{c2}/dT)_{T_c}$ (T/K)	-1.4 -1.4 (scaling)	-2.8 -2.8
$H_{c2}(0)$ (T)	128	226
$\xi_{ab}(0)$ (Å)	16	12

the theoretical value. From this analysis, the Ginzburg-Landau parameter $\kappa_{av} = 110$, the slope of the upper critical field $(dH_{c2}/dT)_{T_c} = -1.4$ T/K, and the zero-temperature upper critical field $H_{c2}(0) = 128$ T were obtained for the pristine sample. The $\kappa_{av} = 117$, $(dH_{c2}/dT)_{T_c} = -2.8$ T/K, and $H_{c2}(0) = 226$ T for the Sr-substituted sample. The obtained slope $(dH_{c2}/dT)_{T_c}$ and the upper critical field $H_{c2}(0)$ for the Sr-substituted sample are about two times that of the nonsubstituted sample. In addition, the substitution of Sr for Ba causes a slight decrease of the magnetic penetration depth $\lambda_{ab}(0)$. The derived various quantities are tabulated in Table I.

The irreversibility line of anisotropic high- T_c superconductor is related to thermal fluctuation. Based on the above analysis, the suppression of the thermal fluctuation was achieved by decreasing the thickness of the charge reservoir block between the superconducting planes. Suppose that the field is perpendicular to the superconducting CuO_2 layers. If the interlayer coupling is relatively strong, the vortex could be well described by 3D lines and the irreversibility line shifts to the higher field and temperature. For the opposite case, the vortex becomes decoupled 2D ‘‘pancake’’ vortices and the irreversibility line is located in a low position. Figure 8 shows the irreversibility lines of the two compounds, along with that of the parent $\text{HgBa}_2\text{Ca}_2\text{Cu}_3\text{O}_{8.5}$.¹⁹ The irreversibil-

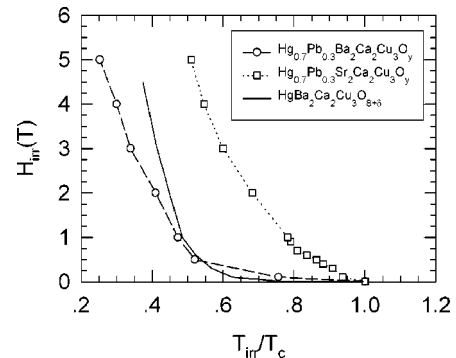


FIG. 8. Irreversibility lines in terms of reduced temperature T_{irr}/T_c , the data of Hg-1223 is from Ref. 19.

ity temperature $T_{\text{ir}}(H)$ is estimated from the merging point of the zero-field-cooled and field-cooled magnetization curve. As shown in Fig. 8, in the low-field range ($H < 0.5$ T), the irreversibility line of $\text{Hg}_{0.7}\text{Pb}_{0.3}\text{Ba}_2\text{Ca}_2\text{Cu}_3\text{O}_y$ is located in a slightly higher position compared to that of the parent Hg-1223. With an increasing field ($H > 0.5$ T), the reversed position is shown. However, the irreversibility region of the Sr-substituted sample is significantly wider compared to that of the nonsubstituted $\text{Hg}_{0.7}\text{Pb}_{0.3}\text{Ba}_2\text{Ca}_2\text{Cu}_3\text{O}_y$ and the host $\text{HgBa}_2\text{Ca}_2\text{Cu}_3\text{O}_y$.

This relatively higher position of the irreversibility line in the $H-T$ phase diagram can be explained by taking into account the enhanced interlayer coupling between the superconducting planes due to the reduction of the c -axis parameter.

It is apparent that the slope $(dH_{c_2}/dT)_{T_c}$ and the upper critical field $H_{c_2}(0)$ are significantly increased by Sr substitution. The significantly enhanced upper critical field and a shift of the irreversibility line to a higher field indicate that $\text{Hg}_{0.7}\text{Pb}_{0.3}\text{Sr}_2\text{Ca}_2\text{Cu}_3\text{O}_y$ compound is very attractive for practical application.

IV. CONCLUSION

We investigated high-field magnetization with applied fields along the c axis for $\text{Hg}_{0.7}\text{Pb}_{0.3}\text{Ba}_2\text{Ca}_2\text{Cu}_3\text{O}_y$ and $\text{Hg}_{0.7}\text{Pb}_{0.3}\text{Sr}_2\text{Ca}_2\text{Cu}_3\text{O}_y$ compositions. At the critical region, the magnetization displayed a good 2D scaling behavior for both compounds. The increase of the interlayer coupling or the suppression of fluctuation was observed for the Sr substituted sample. These phenomena are supported by the measured irreversibility lines and analysis of $\kappa(T)$ near T_c . Based on three different theoretical analysis, the effects of Sr-substitution on the superconducting properties were studied. Especially, a significantly enhanced upper critical field $H_{c_2}(0)$ is revealed in the Sr substituted compounds.

ACKNOWLEDGMENT

This work was supported by the Ministry of Science and Technology of Korea through the Creative Research Initiative Program.

*Also at Department of Physics, Shenyang Normal University, Shenyang 110031, P. R. China.

¹C. W. Chu, L. Gao, F. Chen, Z. J. Huang, R. L. Meng, and Y. Y. Xue, *Nature* (London) **365**, 323 (1993).

²U. Welp, G. W. Crabtree, J. L. Wagner, and D. G. Hinks, *Physica C* **218**, 373 (1993).

³H. M. Shao, C. C. Lam, P. W. C. Fung, X. S. Wu, J. H. Du, G. J. Shen, J. C. L. Chow, S. L. Ho, K. C. Hung, and X. X. Yao, *Physica C* **246**, 207 (1995).

⁴Kazuyuki Isawa, Ayako Tokiwa-Yamamoto, Makato Itoh, Seiji Adachi, and H. Yamauchi, *Appl. Phys. Lett.* **65**, 2105 (1994).

⁵Z. Iqbal, T. Datta, D. Kirven, A. Lungu, J. C. Barry, F. J. Owens, A. G. Rinzler, D. Yang, and F. Reidinger, *Phys. Rev. B* **49**, 12 322 (1994).

⁶K. Kishio, J. Shimoyama, A. Yoshikawa, K. Kitazawa, O. Chmaissem, and J. D. Jorgensen, *J. Low Temp. Phys.* **105**, 1359 (1996).

⁷D. H. Kim, K. E. Gray, R. T. Kampwirth, J. C. Smith, D. S. Richeson, T. J. Marks, J. H. Kang, J. Talvacchio, and M. Eddy, *Physica C* **177**, 431 (1991).

⁸J. L. Tallon, G. V. M. Williams, C. Bernhard, D. M. Pooke, M. P. Staines, J. D. Johnson, and R. H. Meinhold, *Phys. Rev. B* **53**, R11 972 (1996).

⁹Sergey Lee, N. P. Kiryakov, D. A. Emelyanov, M. S. Kuznetsov, Yu. D. Tretyakov, V. V. Petrykin, M. Kakihana, H. Yamauchi, Yi Zhuo, Mun-Seog Kim, and Sung-Ik Lee, *Physica C* **305**, 57 (1998).

¹⁰Sergey Lee, Maxim Kuznetsov, Nikolai Kiryakov, Denis Emelyanov, and Yurii Tretyakov, *Physica C* **290**, 275 (1997).

¹¹O. Chmaissem, J. D. Jorgensen, K. Yamaura, Z. Hiroi, M. Takanano, J. Shimoyama, and K. Kishio, *Phys. Rev. B* **53**, 14 647 (1996).

¹²J. R. Clem, *Phys. Rev. B* **43**, 7837 (1991).

¹³S. Ullah and A. T. Dorsey, *Phys. Rev. Lett.* **65**, 2066 (1990).

¹⁴L. N. Bulaevskii, M. Ledvij, and V. G. Kogan, *Phys. Rev. Lett.* **68**, 3773 (1992).

¹⁵A. E. Koshelev, *Phys. Rev. B* **50**, 506 (1994).

¹⁶Zhidong Hao, John R. Clem, M. W. McElfresh, L. Civale, A. P. Malozemoff, and F. Holtzberg, *Phys. Rev. B* **43**, 2844 (1991).

¹⁷R. Puźniak, R. Usami, K. Isawa, and H. Yamauchi, *Phys. Rev. B* **52**, 3756 (1995).

¹⁸Yi Zhuo, Jae-Hyuk Choi, Mun-Seog Kim, Wan-Seon Kim, Z. S. Lim, Sung-Ik Lee, and Sergey Lee, *Phys. Rev. B* **55**, 12 719 (1997).

¹⁹Y. C. Kim, J. R. Thompson, D. K. Christen, Y. R. Sun, M. Paranthaman, and E. D. Specht, *Phys. Rev. B* **52**, 4438 (1995).